JOURNAL

OF THE AMERICAN CHEMICAL SOCIETY

VOLUME 106, NUMBER 16 AUGUST 8, 1984

Mechanism of the Reaction of Gas-Phase Iron Ions with Neutral Olefins

D. A. Peake,[†] M. L. Gross,*[†] and D. P. Ridge*[‡]

Contribution from the Chemistry Department, University of Nebraska, Lincoln, Nebraska 68588, and the Chemistry Department and Center for Catalytic Science and Technology, University of Delaware, Newark, Delaware 19711. *Received December 1, 1983*

Abstract: The structures of $FeC_nH_{2n}^+$ species formed by reaction of $Fe(CO)^+$ with olefins (n = 2–14) and cycloalkanes (n = 3–6) in a high-pressure source were examined by using mass spectrometric techniques. The stoichiometry of the complexes was confirmed by high-resolution mass spectrometry, and their structures were probed by collisional activation of the iron–olefin complex in a tandem mass spectrometer (MS/MS). Ethylene, propene, and isobutene retain their structural integrity in complexes with Fe^+, but all of the other olefins studied rearrange after complexation to a structure with two or more ligands. These rearrangements are generally consistent with a mechanism that begins with addition of an allylic C–C bond to the metal ion followed by abstraction of a β-H atom from the resulting alkyl ligand to form a hydrido π-allyl intermediate. Transfer of the H atom to the allylic fragment produces a bis(olefin) complex. This mechanism dominates unless the required β-H is absent. Possible alternatives to this mechanism are presented for intermediates with no available β-hydrogen. Additional support for the mechanism was obtained by studying the structures of decomposition products of the $FeC_nH_{2n}^+$ adducts. These studies involved comparisons of the collision-activated decomposition (CAD) spectra of product ions formed either in the source by bimolecular reactions or by collisional activation of stable $FeC_nH_{2n}^+$ (an MS/MS/MS experiment) with corresponding reference spectra. Finally, the generality of the allylic insertion mechanism was tested by examining a series of $FeC_8H_{16}^+$ ions formed from isomeric octenes and methylheptenes.

The activation of C–H and C–C bonds of hydrocarbons by transition-metal complexes is of fundamental interest in catalysis and has attracted considerable attention. While the direct activation of C–H bonds by an intermolecular process has been observed in solution only recently,[1] the activation of C–C and C–H bonds by gas-phase metal ions has been demonstrated repeatedly over the last 5 years. The first evidence of the oxidative addition of an alkyl halide[2] and a hydrocarbon[3] to a gas-phase metal ion was obtained by ion cyclotron resonance (ICR) studies. Fe^+, generated by electron ionization of $Fe(CO)_5$, reacted with isobutane to give both C–C and C–H bond insertion followed by β-H transfer and reductive elimination. Since then a variety of gas-phase metal ions have been shown to react with alkanes,[4-12] alkenes and cycloalkanes,[13-16] ketones,[17-19] and alcohols.[20]

The advantage of studying organometallic reactions in the gas phase is there are no solvent effects to complicate or mask the reaction mechanism. Methods which have been employed to study gas-phase metal ion chemistry include ICR,[21] Fourier transform mass spectrometry (FTMS),[22] ion beam apparatus,[23] and collision-activated decomposition (CAD) spectroscopy.[24] Elucidation of reaction mechanisms may be facilitated by determination of product ion structures. Although the chemical reactivity of an ion can reveal some of its structural features, high energy CAD spectroscopy frequently provides a more distinctive and informative picture of ion structure. Also, the CAD experiment can often be done more expeditiously. The CAD process occurs when a mass-selected ion collides with an inert gas which transfers internal

[†] University of Nebraska.
[‡] University of Delaware.

(1) Haggin, J. *Chem. Eng. News* **1982**, Feb 14, 9.
(2) Allison, J.; Ridge, D. P. *J. Organomet. Chem.* **1975**, *99*, C11–14.
(3) Allison, J.; Freas, R. B.; Ridge, D. P. *J. Am. Chem. Soc.* **1979**, 101, 1332.
(4) Freas, R. B.; Ridge, D. P. *J. Am. Chem. Soc.* **1980**, *102*, 7129.
(5) Armentrout, P. B.; Beauchamp, J. L. *J. Am. Chem. Soc.* **1980**, *102*, 1736.
(6) Armentrout, P. B.; Beauchamp, J. L. *J. Am. Chem. Soc.* **1981**, 103, 784.
(7) Byrd, G. D.; Burnier, R. C.; Freiser, B. S. *J. Am. Chem. Soc.* **1982**, *104*, 3565.
(8) Byrd, G. D.; Freiser, B. S. *J. Am. Chem. Soc.* **1982**, *104*, 5944.
(9) Halle, L. F.; Houriet, R.; Kappes, M.; Staley, R. H.; Beauchamp, J. L. *J. Am. Chem. Soc.* **1982**, *104*, 6293.
(10) Jacobsen, D. B.; Freiser, B. S. *J. Am. Chem. Soc.* **1983**, *105*, 736.
(11) Jacobsen, D. B.; Freiser, B. S. *J. Am. Chem. Soc.* **1983**, *105*, 5197.
(12) Larsen, B.; Ridge, D. P. *J. Am. Chem. Soc.* **1984**, *106*, 1912–1922.
(13) Allison, J.; Ridge, D. P. *J. Am. Chem. Soc.* **1977**, *99*, 35.
(14) Armentrout, P. B.; Halle, L. F.;Beauchamp, J. L. *J. Am. Chem. Soc.* **1981**, *103*, 6624.
(15) Armentrout, P. B.; Beauchamp, J. L. *J. Am. Chem. Soc.* **1981**, *103*, 6628.
(16) Jacobsen, D. B.; Freiser, B. S. *J. Am. Chem. Soc.* **1983**, *105*, 7484.
(17) Ridge, D. P.; Allison J. "26th Annual Conference of Mass Spectrometry and Allied Topics"; 1978; p 224.
(18) Burnier, R. C.; Byrd, G. D.; Freiser, B. S. *Anal. Chem.* **1980**, *52*, 1641.
(19) Burnier, R. C.; Byrd, G. D.; Frieser, B. S. *J. Am. Chem. Soc.* **1981**, *103*, 4360.
(20) Allison, J.; Ridge, D. P. *J. Am. Chem. Soc.* **1979**, *101*, 4998.

0002-7863/84/1506-4307$01.50/0

energy to the ion, causing fragmentation. The resulting spectrum contains structural information about the selected ion.

The CAD process is observed at high kinetic energies (3–20 keV) by using mass-analyzed ion kinetic energy spectrometry (MIKES) with reversed geometry (B–E) instruments.[25,26] High-energy CAD has been applied to the study of $Fe(C_4H_{10})^+$ and $Cr(C_4H_{10})^+$ product ions formed by reaction of the ionized metal carbonyl with isobutane in a chemical ionization (CI) source[4] and to the study of reactions of Fe^+ with alkanes, and alkenes.[12] Low-energy (<100 eV) CAD spectroscopy has recently been demonstrated by using triple quadrupole[27] and FT mass spectrometers.[28] The reactions of Ni^+, Co^+, and Fe^+ with alkanes were investigated by using the collisional activation (CA) capabilities of FTMS.[10,11]

We report here a high-energy CAD spectroscopic study of reactions of Fe^+ with isomeric alkenes and cycloalkanes. This work and the previous CAD studies[4,10-12] of gas-phase metal ion complexes provide the first clear demonstration of the merit of CAD for determination of the structure of metal ion complexes and for inference of reaction mechanisms. Furthermore, we illustrate the advantage of determining the structure of product ions formed by decomposition of Fe–olefin$^+$ complexes as an additional test of mechanism. The structures of these product ions were investigated by CA of the intermediates formed in the ion source and verified by using the consecutive reaction technique[29] (MS/MS/MS) described in the Experimental Section. A practical spinoff of this mechanistic study is the demonstration that double bonds in isomeric olefins can be located by interpreting the CAD spectra of the iron–olefin complexes.

This paper is organized in two parts. We have chosen isomeric C_8H_{16} olefins as a model system for a deductive test of a mechanism involving preferential allylic insertion of Fe^+ into the neutral olefin. This hypothesis is tested in the second half of the paper. As a prelude, we present and interpret the CAD spectra of the smaller Fe–Olefin$^+$ complexes beginning with $FeC_2H_4^+$ and extending to $FeC_6H_{12}^+$. These CAD spectra serve as the necessary references for the determination of the decomposition product ion structures. In addition, the complexes of small olefins and cycloalkanes with Fe^+ have been investigated since metallocycle and carbenoid structures have been suggested to form in the reactions of Co^+ with cycloalkanes and alkenes.[15,23]

Experimental Section

All CAD experiments were performed on a Kratos MS50 triple-analyzer mass spectrometer[30] which consists of a Nier–Johnson geometry high-resolution mass spectrometer followed by an electrostatic analyzer (ESA) (Figure 1). The ions formed in the source were mass selected at a mass resolution of 6000–8000 (10% valley definition) using MS-I (ESA-1 and magnet). The metal ion complex was then activated by collisions with helium gas in the second collision cell. The second ESA is scanned to give the CAD spectrum of the resulting fragment ions. In a typical CAD experiment 10–20 scans were acquired and signal averaged by using software written in this laboratory. The precision for all peak heights reported was approximately ±10% relative as determined by replicate experiments performed several months apart.

Consecutive reaction experiments were performed in a manner described previously.[29] The metal complex (M_1^+) was dissociated by reaction in collision cell 1 located between the ion source and ESA-1. When the voltage on ESA-1 is adjusted by the ratio M_2/M_1 and M_2^2/M_1 is selected with the magnet, M_2^+ is passed by MS-I and collisionally activated in collision cell 2 (see reaction 1).

$$M_1^+ \xrightarrow[\text{CAD}]{} M_2^+ \xrightarrow[\text{CAD}]{} \text{product ions} \qquad (1)$$

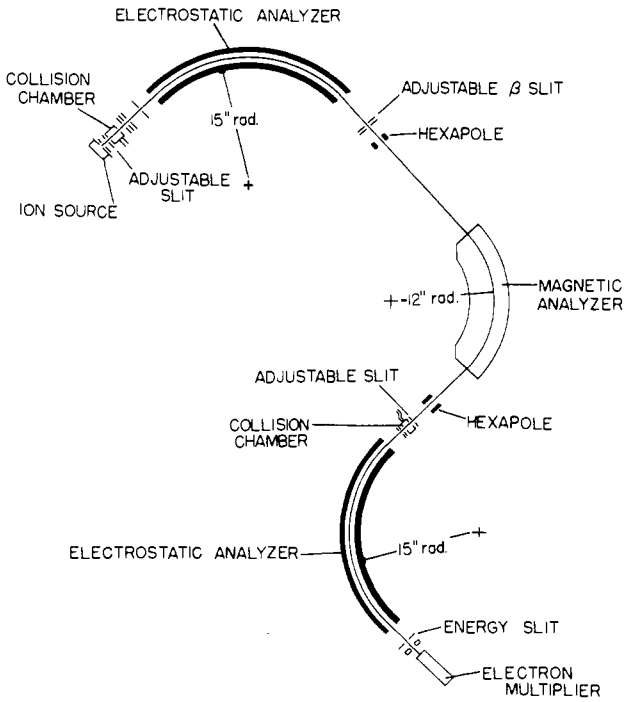

Figure 1. Ion optics of the Kratos MS-50 triple analyzer. (Reprinted with permission from *Int. J. Mass Spectrom. Ion Phys.* Copyright 1982, Elsevier.)

The $Fe(C_nH_{2n})^+$ ions were formed by ion–molecule reactions in the CI source between $Fe(CO)^+$, an ionic decomposition product of $Fe(CO)_5^+$, and the appropriate alkene. $Fe(CO)_5$ (30 μL) was injected into an 80-mL all-glass reservoir probe which was inserted through the solid's vacuum lock to contact a source entrant. The flow of $Fe(CO)_5$ into the source was regulated by a 7.5-cm long capillary restriction which gave a pressure of $2–5 \times 10^{-6}$ torr in the source housing as measured by an ion gauge. The alkene (10 μL) was admitted through a heated inlet, bringing the total pressure to $5 \times 10^{-4} - 1 \times 10^{-3}$ torr (~0.5–1.0 torr in the source). The source pressure was estimated by comparison of pressures measured by a Hastings gauge vs. the source housing pressure using methane as the calibrant gas. The Hastings gauge was mounted on a probe which was inserted through the vacuum lock.

The CI source was operated at 280-eV ionization energy with a total emission current of 500 μA. The repeller was set to 0 V with respect to the source chamber. The ion accelerating voltage was 8000 V. The source temperature was reduced to 100 °C to minimize the thermal decomposition of $Fe(CO)_5$. CAD spectra were acquired after 50% suppression of the selected ion beam using helium as the collision gas.

Full-scan high-resolution (R = 10000) spectra of the $Fe(CO)_5$/alkene mixtures were acquired with a Kratos MS50 double focusing mass spectrometer interfaced to a Nova-4X computer and processed with DS-55 software. The CI source was operated under the same conditions as in the CAD experiments. Perfluorokerosene (PFK) was introduced via a heated inlet, bringing the source housing pressure to 5×10^{-5} torr. Calibration from m/z 50 to m/z 800 was achieved at a scan rate of 10 s/decade of mass in a typical run. $Fe(CO)_5$ and the alkene (30 μL each) were injected into the reservoir probe bringing the total pressure to $1–2 \times 10^{-5}$ torr (~10 mtorr in the source).

The octene and methylheptene isomers, purchased from Wiley Organics (Columbus, OH) and reported to be >99% pure, were used without further purification. Iron pentacarbonyl was purchased from Strem Chemicals (Newburyport, MA).

Results and Discussion

In order to investigate the reactions of Fe^+ with alkenes in the gas phase, a suitable source of gas-phase metal ions is necessary. Iron pentacarbonyl was chosen for its high volatility and well-characterized gas-phase chemistry. The electron impact mass spectrum of $Fe(CO)_5$ is dominated by the $Fe(CO)^+$ ion formed by consecutive losses of CO from the molecular ion. Under high pressure or CI conditions, $Fe(CO)_5^+$ (m/z 196) becomes the base peak, and ion-molecule reactions produce ions greater than mass 196. Elemental compositions of the product ions, assigned from high-resolution exact mass measurements (Table I), agree with those of Foster and Beauchamp, who made use of low-mass

(21) Baldeschwieler, J. D. *Science (Washington, D.C.)* **1968**, *159*, 263.
(22) Wilkins, C. L.; Gross, M. L. *Anal. Chem.* **1981**, *53*, 1661A.
(23) Armentrout, P. B.; Beauchamp, J. L. *J. Chem. Phys.* **1981**, *74*, 2819.
(24) Levson, H.; Schwarz, H. *Angew. Chem., Int. Ed. Engl.* **1976**, *15*, 509.
(25) Beynon, J. H.; Cooks, R. G.; Amy, J. W.; Baitinger, E.; Ridley, T. Y. Anal. *Chem.* **1973**, *45*, 1023A.
(26) Kondrat, R. W.; Cooks, R. G. *Anal. Chem.* **1978**, *50*, 81A.
(27) Enke, C. G.; Yost, R. A. *Anal. Chem.* **1979**, *51*, 1251A.
(28) Cody, R. B.; Burnier, R. C.; Freiser, B. S. *Anal. Chem.* **1982**, *54*, 96.
(29) Burinsky, D. J.; Cooks, R. G.; Chess, E. K.; Gross, M. L. *Anal. Chem.* **1982**, *54*, 295.
(30) Gross, M. L.; Chess, E. K.; Lyon, P. A.; Crow, F. W.; Evans, S.; Tudge, H. *Int. J. Mass Spectrom. Ion Phys.* **1982**, *42*, 243.

Table I. $Fe(CO)_5$ Ion–Molecule Products

measured mass	formula	ppm[a]	% RA
447.7556	$Fe_3(CO)_{10}$	3.7	0.3
391.7642	$Fe_3(CO)_8$	0.3	0.5
363.8230	$Fe_2(CO)_9$	−3.0	0.2
363.7701	$Fe_3(CO)_7$	2.6	0.8
335.8296	$Fe_2(CO)_8$	1.3	1.4
307.8347	$Fe_2(CO)_7$	1.3	1.4
279.8398	$Fe_2(CO)_6$	1.5	3.4
251.8445	$Fe_2(CO)_5$	0.4	1.9
223.8500	$Fe_2(CO)_4$	2.2	6.9
195.9090	$Fe(CO)_5$	−2.8	100
167.9149	$Fe(CO)_4$	1.6	40.6
139.9194	$Fe(CO)_3$	−2.1	6.1
111.9252	$Fe(CO)_2$	3.7	7.9
83.9299	Fe(CO)	0.5	25.0
55.9361	Fe	20.0	14.0

[a] Mass measurement error in ppm.

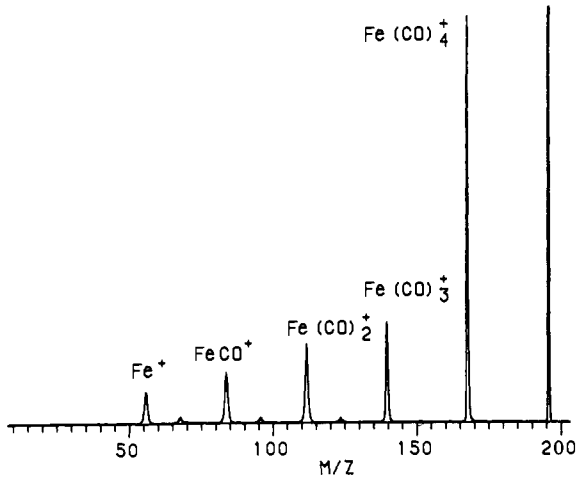

Figure 2. CAD spectrum of $Fe(CO)_5^+$, m/z 196.

resolution ICR spectrometry.[31] The CAD spectrum of $Fe(CO)_5^+$ (Figure 2) verifies that consecutive losses of CO occur from the molecular ion.[32]

The reactions of the ionic decomposition products of $Fe(CO)_5^+$ and alkenes are generalized by reaction 2. In ionized Fe-

$$Fe(CO)_x^+ + C_nH_{2n} \rightarrow Fe(C_nH_{2n})(CO)_{x-1}^+ + CO \quad (2)$$

$(CO)_5$/alkene mixtures, complexes with zero to three carbonyls (x = 1–4) are formed (Table II). In addition to products from reaction 2, other ions were observed. For example, $Fe(C_6H_{12})_2^+$ and $FeC_3H_6^+$ ions formed from 1-hexene and $Fe(CO)_5$ indicate that multiple reactions and fragmentations take place.

A typical CAD experiment can be illustrated by consideration of the Fe(1-hexene)$^+$ complex. The $FeC_6H_{12}^+$ ions produced in reaction 1 (x = 1) were separated from isobaric $Fe(CO)_3^+$ by using MS-I and collisionally activated with He target gas in the second collision cell (Figure 1). The spectrum of the resulting fragments (Figure 3) shows that the most intense CAD fragment is $FeC_3H_6^+$ corresponding to a loss of propene from Fe(1-hexene)$^+$.

The structural evidence provided by high-energy CAD is more direct than that from ion–molecule reactions. For example, in ion beam studies, Co^+ reacted with 1-hexene to give $CoC_3H_6^+$ as the dominant product.[14] A bis(olefin) complex was suggested but not proven to be the intermediate resulting from the cleavage of the allylic C–C bond. The CAD experiment with Fe(1-hexene)$^+$ provides direct evidence that Fe(1-hexene)$^+$ readily assumes a $Fe(propene)_2^+$ structure because the $FeC_3H_6^+$ product of the reaction can be shown to be Fe(propene)$^+$ as discussed below.

$FeC_2H_4^+$, $FeC_3H_6^+$, and $FeC_4H_8^+$. The complexes of Fe^+ with the linear butenes lose H_2 readily to give a butadiene complex.[12] Isobutene remains intact when coordinated to Fe^+. Upon colli-

(31) Foster, M. S.; Beauchamp, J. L. *J. Am. Chem. Soc.* **1975**, *97*, 4808.
(32) Winters, R. E.; Collins, J. H. *J. Phys. Chem.* **1966**, *70*, 2057.

Table II. High-Resolution MS of $Fe(CO)_5$/Alkene Mixtures

alkene	measured mass	formula	ppm[a]	% RA
1-hexene	224.1230	$Fe(C_6H_{12})_2$	1.4	10.8
	224.0136	$Fe(CO)_3C_6H_{12}$	0.0	3.2
	196.0190	$Fe(CO)_2C_6H_{12}$	1.5	8.6
	182.0758	FeC_9H_{18}	0.0	1.3
	168.0204	$Fe(CO)C_6H_{12}$	1.7	4.7
	140.0290	FeC_6H_{12}	1.0	9.6
	97.9820	FeC_3H_6	0.8	6.1
1-heptene	252.1543	$Fe(C_7H_{14})_2$	1.2	2.1
	210.0346	$Fe(CO)_2C_7H_{14}$	1.5	4.1
	182.0394	$Fe(CO)_1C_7H_{14}$	0.3	2.6
	154.0445	FeC_7H_{14}	0.0	6.8
	97.9817	FeC_3H_6	−1.7	1.6
1-octene	224.0499	$Fe(CO)_2C_8H_{16}$	−0.3	1.5
	168.0602	FeC_8H_{16}	0.3	3.3
	126.0132	FeC_5H_{10}	0.0	3.8
	97.9819	FeC_3H_6	0.5	1.1
2-octene	224.0500	$Fe(CO)_2C_8H_{16}$	0.4	1.3
	196.0551	$Fe(CO)_1C_8H_{16}$	0.5	1.4
	168.0601	FeC_8H_{16}	−0.4	2.4
	111.9966	FeC_4H_8	−7.9	2.7

[a] Mass measurement error in ppm.

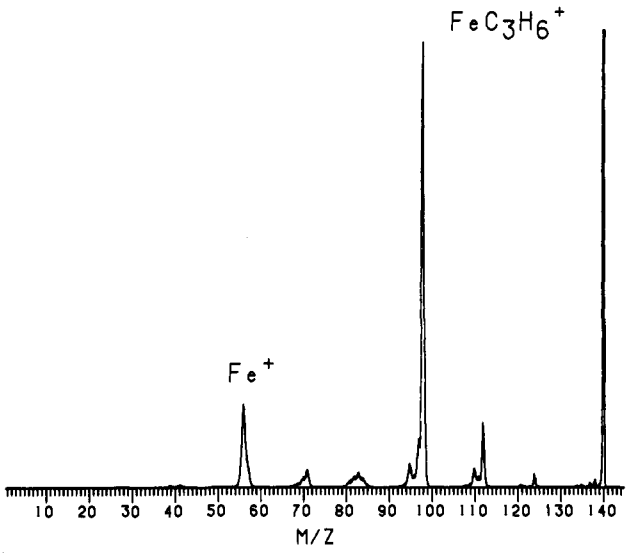

Figure 3. CAD spectrum of Fe(1-hexene)$^+$, m/z 140.

sional activation, the isobutene complex loses predominantly C_4H_8 to form Fe^+ and small amounts of $FeCH_3^+$ and $FeC_3H_4^+$. In contrast to the CAD spectra of $FeC_4H_8^+$ formed from the acyclic C_4H_8 isomers, those of cyclobutane and methylcyclopropane complexes are dominated by $FeC_2H_4^+$ (Table III). On the basis of a comparison of the CAD spectra of the complexes formed from the cyclic C_4H_8's and that of the bis(ethylene) complex, we suggest that three unique structures exist (**1**–**3**). Structure **1** is assigned

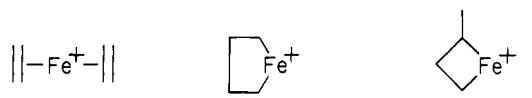

1 **2** **3**

to the $FeC_4H_8^+$ formed by reaction of $Fe(CO)_2^+$ with ethylene.[12] Although the CAD spectrum of the bis(ethylene) complex is quite similar to that of the cyclobutane complex, the loss of H_2 is seven times more intense in the CAD spectrum of Fe(cyclobutane)$^+$. The loss of H_2 is more likely to occur upon collisional activation of **2**, a metallacyclopentane ion. Structure **2** has previously been suggested for the $FeC_4H_8^+$ produced by reaction of cyclopentanone with Fe^+.[11,12] A metallacyclopentane has also been suggested as an intermediate in the reaction of cyclobutane with a cobalt ion beam.[15] However, the CAD spectrum of $FeC_4H_8^+$ from cyclopentanone appears to be a 1:1 linear combination of the Fe(1-

Table III. CAD Spectra of $FeC_4H_8^+$

hydrocarbon	fragment ions											
	FeC_4H_6	FeC_3H_5	FeC_3H_4	FeC_3H_3	FeC_2H_4	FeC_2H_3	FeC_2H_2	FeC_2H	$FeCH_3$	$FeCH_2$	FeH	Fe
cyclobutane	28.9	0.6	0.6	1.2	100.0	16.0	3.1	2.5	1.8	5.5		36.9
methylcyclopropane	48.5	1.2[a]	1.2	2.5	100.0	8.6	1.5	1.9	4.3	13.6	9.3	32.1
$(ethylene)_2$[b]	4.3				100.0	12.6	4.9	4.0	0.6	4.9	11.7	29.5
1-butene	100.0	0.8	0.6	1.3	0.7	3.9	1.0	1.1	1.9	1.0	3.8	15.1
cis-2-hexene	100.0	0.6	0.6	1.5	1.1	4.6	1.2	1.2	2.5	0.6	4.9	20.4
cis-3-hexene	100.0	0.6	0.6	1.3	0.6	4.2	1.0	1.3	2.3	0.6	4.5	18.1
cis-3-methyl-2-pentene	100.0	0.6	0.6	1.8	0.6	4.6	1.5	1.2	2.5	1.2	4.9	19.6
1-heptene	100.0	0.9	0.7	1.4	1.0	4.1	1.0	1.4	2.1	1.0	4.8	17.6
trans-2-octene	100.0	0.6	0.6	1.2	0.9	4.3	1.2	1.2	2.1	0.9	4.3	15.9
2-methyl-1-heptene	100.0	1.9	8.9	5.7	1.9	8.9	3.2	4.4	12.7	3.8		71.5
isobutene	4.1		22.2	7.2		3.5	1.6	3.8	17.2	5.1		100.0
2-methyl-1-pentene	13.2	1.4	21.6	9.5	0.7	4.7	2.0	4.1	22.3	4.7		100.0
2-methyl-2-pentene	1.9	1.2	24.1	9.3		4.3	1.9	4.3	21.0	5.6		100.0

[a] $FeC_3H_6^+$, 1.2 % RA. [b] Formed by reaction of $Fe(CO)_2^+$ with ethylene.[12]

Table IV. CAD Spectra of $FeC_2H_4^+$

hydrocarbon	fragment ions										
	FeC_2H_3	FeC_2H_2	FeC_2H	FeC_2	$FeCH_2$	FeCH	FeC	FeH	Fe	$FeC_2H_4^{2+}$	C_2H_4
ethylene	8.2	4.5	6.7	0.7	2.3	2.6	2.5	13.4	100	2.1	0.3
methylcyclopropane	10.5	5.6	8.0	1.2	1.9	2.5	2.2	14.5	100	2.5	0.3
cyclobutane	8.6	4.9	7.4	1.2	2.5	2.8	2.5	13.5	100	1.5	0.3

Table V. CAD Spectra of $FeC_3H_6^+$

olefin	fragment ions													
	Fe-C_3H_5	Fe-C_3H_4	Fe-C_3H_3	Fe-C_3H_2	FeC_3H	Fe-C_2H_3	Fe-C_2H_2	FeC_2H	$FeCH_3$	$FeCH_2$	FeCH	FeC	Fe	C_3H_3
cyclopropane	0.6	0.6	11.8	1.9	1.2	1.9	3.1	3.7	4.3	70.2	7.8	4.3	100	1.2
propene	1.9	2.2	10.7	0.8	0.8	2.4	3.5	4.4	5.1	4.2	1.6	1.6	100	1.1
1-hexene	4.0	1.7	13.4	1.3	1.3	2.3	3.0	4.7	6.0	4.7	2.0	1.3	100	1.3
1-pentene	3.7	2.2	16.9	1.5	1.5	2.6	3.7	4.8	7.4	5.1	2.9	1.5	100	1.5
2-methyl-1-butene	4.8	1.9	14.9	0.6	0.6	2.3	2.6	4.9	6.5	5.5	2.6	1.3	100	1.3
3-methyl-1-butene	5.6	3.2	22.6	2.0	1.6	2.4	4.0	4.8	7.2	6.5	3.2	1.6	100	1.3
2-methyl-2-butene	5.9	3.7	14.7	1.5	1.5	2.2	3.7	5.1	8.8	4.4	2.2	1.5	100	1.5

butene)$^+$ and Fe(cyclobutane)$^+$ spectra, suggesting a mixture of ion structures is formed in the reaction of Fe^+ with cyclopentanone.

A metallacyclobutane ion, **3**, is postulated for $FeC_4H_8^+$ formed by reaction of Fe^+ with methylcyclopropane. A metallacyclobutane has been suggested by Beauchamp et al. to be the intermediate in the reaction of cyclopropane with a Co^+ beam to produce $Co{=}CH_2^+$.[15] A similar intermediate, **3**, wouuld be consistent with the collisionally activated loss of C_2H_4 from Fe(methylcyclopropane)$^+$ (Scheme I). Oxidative addition of Fe^+ into the C–C bond adjacent to the methyl group followed by elimination of ethylene would result in the formation of $FeC_2H_4^+$.

In addition, $Fe{=}CH_2^+$ formed by loss of C_3H_6 from **3** is more pronounced in the CAD spectrum of **3** than in the spectra of **1** and **2**. This carbene complex may occur via **3** or by insertion of Fe^+ into the methyl bond of methylcyclopropane.

The CAD spectra of $FeC_2H_4^+$ formed in the CI source from the two cyclic C_4H_8 isomers (Table IV) are nearly identical with that of Fe(ethylene)$^+$, suggesting the $FeC_2H_4^+$ fragments have an Fe(ethylene)$^+$ structure. The loss of C_2H_4 dominates the Fe(ethylene)$^+$ CAD spectrum. Other features are the loss of three hydrogens, perhaps giving a Fe—C≡C—H$^+$ structure, and a significant charge stripping peak (reaction 3).

$$FeC_2H_4^+ + He \rightarrow Fe(C_2H_4)^{+2} + He + e- \quad (3)$$

The CAD spectra of the $FeC_3H_6^+$ from the reaction of propene or cyclopropane with $Fe(CO)^+$ are indicative of two unique structures for this ion (Table V) (**4** and **5**). Propene probably

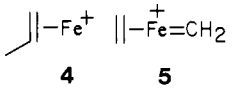

4 **5**

retains its structure when bound to Fe^+, as indicated by **4**, because collisional activation of **4** produces principally Fe^+. On the other hand, cyclopropane probably forms complex **5** with carbene and ethylene ligands attached to the metal. This occurs by rearrangement of a metallacyclobutane intermediate by a mechanism similar to Scheme I. Upon collisional activation, the intermediate loses neutral C_2H_4 to form $Fe{=}CH_2^+$, which is expected for **5**.

Scheme I

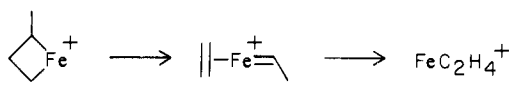

3

$FeC_5H_{10}^+$. A comparison of CAD spectra of the C_5H_{10} complexes (Table VI) with complexes of the smaller olefins reveals that new decomposition reactions are being observed. All of the $FeC_5H_{10}^+$ adducts lose ethylene, indicating C–C bond cleavage is becoming an important dissociation pathway (reaction 4). In

$$FeC_5H_{10}^+ \rightarrow FeC_3H_6^+ + C_2H_4 \quad (4)$$

contrast, the complexes formed from ethylene, propene, and the acyclic butenes predominantly lose H_2 or the alkene while little C–C bond cleavage is observed. Although FeC_5H_{10} ions principally dissociate according to reaction 4, the loss of H_2 is significantly different for complexes of each C_5H_{10} isomer, indicating that different structures exist.

The $FeC_3H_6^+$ ions produced in the source by reaction of Fe^+ with the C_5H_{10} isomers gave the same CAD spectra as the $FeC_3H_6^+$ ions from propene (Table V). In order to characterize unequivocally the $FeC_3H_6^+$ ions produced specifically by collisional activation of $FeC_5H_{10}^+$, the consecutive reaction experiment (MS/MS/MS) described in the Experimental Section was conducted. The partial CAD spectrum of $FeC_3H_6^+$ formed in the source by decomposition of Fe(1-pentene)$^+$ is identical (Figure 4) to the spectrum of the $FeC_3H_6^+$ formed uniquely by CA of

Table VI. CAD Spectra of $FeC_5H_{10}^+$

	fragment ions															
hydrocarbon	Fe-C_5H_8	Fe-C_5H_7	Fe-C_5H_6	Fe-C_5H_5	Fe-C_4H_6	Fe-C_4H_4	Fe-C_3H_6	Fe-C_3H_5	Fe-C_3H_3	Fe-C_2H_4	Fe-C_2H_3	Fe-C_2H_2	Fe-C_2H	Fe-CH_3	Fe-CH_2	Fe
1-pentene	4.5	1.4		0.9	8.1		100.0	7.4	3.8	20.7	4.4	2.7	1.3	3.4	2.4	20.0
1-octene	5.0	1.4		1.1	12.1		100.0	8.2	3.6	20.2	4.3	3.6	1.4	3.6	1.8	19.3
trans-2-pentene	24.5	2.3		1.7	52.4	0.6	100.0	6.0	4.6	18.2	4.0	3.8	1.6	5.4	1.8	20.6
cis-2-pentene	25.4	2.8		1.5	51.8	0.6	100.0	5.9	4.0	17.5	4.5	4.2	1.9	5.3	1.8	19.4
trans-3-octene	12.9	1.7		1.4	28.6	0.7	100.0	6.8	4.1	18.7	4.4	2.7	1.4	5.4	1.4	21.1
cis-3-octene	14.3	2.2		0.7	30.9	0.7	100.0	6.6	5.1	19.1	4.4	5.1	1.5	4.0	1.8	20.6
2-methyl-1-butene	56.9	2.2	0.9	1.2	73.1	3.3	100.0	8.1	5.5	18.9	4.5	4.3	2.9	6.9	2.7	29.3
3-methyl-3-heptene	63.8	4.3		1.2	81.0	4.6	100.0	9.8	5.5	19.6	5.5	4.3	2.1	7.7	3.1	31.9
3-methyl-1-butene	40.4	2.9		1.4	64.2	2.4	100.0	7.4	5.3	18.2	5.9	4.0	1.7	6.4	2.0	25.7
2-methyl-2-butene	51.8	2.9		1.4	65.3	3.0	100.0	7.6	4.7	17.5	4.5	3.9	2.5	6.4	3.5	24.7
2-methyl-2-heptene	54.2	3.1		1.7	77.1	2.8	100.0	8.3	5.2	19.4	4.9	4.9	2.1	6.9	2.1	26.0
cyclopentane	100.0		40.7	14.5	1.7		3.7	1.7	2.4	1.9		1.2			1.9	22.3

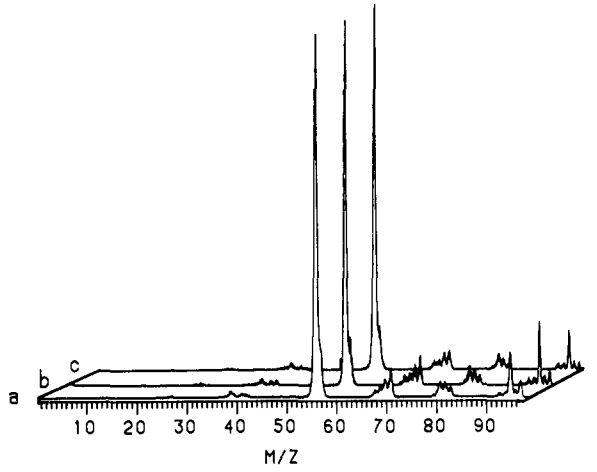

Figure 4. CAD spectra of $FeC_3H_6^+$, m/z 98, from (a) MS/MS/MS of Fe(1-pentene)$^+$, (b) $FeC_3H_6^+$ formed in the source from 1-pentene, and (c) Fe(propene)$^+$.

Scheme II

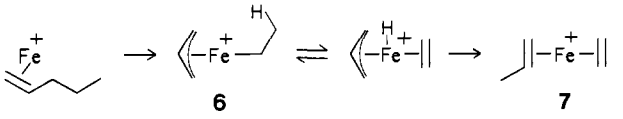

6 **7**

Fe(1-pentene)$^+$ and with the spectrum of Fe(propene)$^+$. This result is in accord with a mechanism proposed by Beauchamp et al. for the reaction of Co^+ with 1-pentene.[14] The oxidative addition of Fe^+ to the allylic C–C bond results in **6**, an intermediate with an alkyl ligand that has a β-hydrogen (Scheme II). Fast β-hydrogen transfer to the metal and back to the allyl ligand results in **7**, a bis(olefin) complex. Collisional activation of **7** causes loss of the smaller olefin, giving Fe(propene)$^+$, since larger alkenes are bound more strongly to the metal center.[33] This new mechanism is not observed for reaction of alkenes with less than five carbons because intermediates corresponding to **6** would not have β-hydrogens available for transfer.

The CAD spectra of the 2-pentene and methylbutene complexes are dominated by the loss of C_2H_4, but pronounced losses of CH_4 and H_2 are also observed. Since the loss of ethylene from these complexes is not expected from the allylic insertion mechanism described above, alternate mechanisms must be proposed to account for the observed products. The loss of ethylene from Fe(2-pentene)$^+$ is best explained by the isomerization of 2-pentene to 1-pentene followed by the allylic insertion mechanism shown in Scheme II (Scheme III). The oxidative addition of the allylic C–H bond to Fe^+ results in **8**, a hydrido π-allyl intermediate. Transfer of the H atom to the substituted end of the allyl ligand results in the formation of Fe(1-pentene)$^+$. The loss of H_2 can

(33) Kappes, M.; Staley, R. H. *J. Am. Chem. Soc.* **1982**, *104*, 1813.

Scheme III

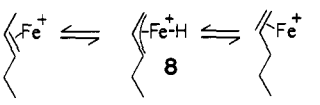

8

Scheme IV

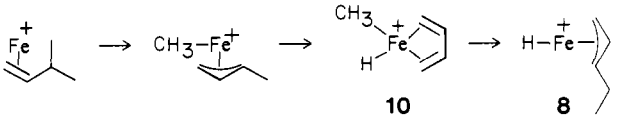

10 **8**

also be rationalized by this mechanism. Insertion of Fe^+ into a second allylic C–H bond of **8** results in **9**, a dihydrido pentadiene species which should lose H_2 to form Fe(1,3-pentadiene)$^+$.

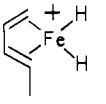

9

The loss of CH_4 from Fe(2-pentene)$^+$ is postulated to occur by insertion of Fe^+ into the allylic C–C bond followed by a H transfer via a six-membered transition state (see below). The $FeC_4H_6^+$ formed by decomposition of Fe(2-pentene)$^+$ in the source has a CAD spectrum which is identical with that of the butadiene complex.[12]

The methylbutene complexes upon collisional activation give more H_2 and CH_4 losses than the linear pentene complexes. The loss of methane may occur by the mechanism shown in Scheme IV. Oxidative addition of the allylic C–C bond followed by transfer of a H atom from the allyl ligand results in **10**. Reductive elimination of CH_4 from **10** would result in formation of Fe(butadiene)$^+$. The dominant loss of ethylene may be explained by rearrangement of the olefin ligand to a linear structure via **10**. The transfer of the methyl ligand back to the butadiene would result in formation of a hydrido π-allyl intermediate, structure **8** in Scheme III, which rearranges to a linear $FeC_5H_{10}^+$ with subsequent loss of ethylene as discussed above. Alternatively, the insertion into the allylic C–H bond of the methylbutene complex could result in the formation of a dihydrido isoprene complex which should readily lose H_2.

The reactions of the Fe(cyclopentane)$^+$ adduct differ markedly from reactions observed for the olefin complexes. Reactions 5 and 6 involving dehydrogenation dominate the CAD spectra. The

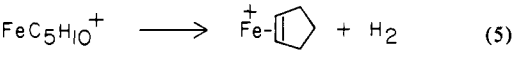

(5)

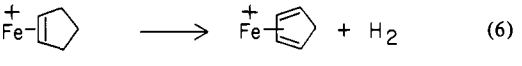

(6)

Table VII. CAD Spectra of $FeC_5H_8^+$ and $FeC_5H_6^+$ from Cyclopentane

hydrocarbon	fragment ions							
	FeC_5H_6	FeC_5H_5	FeC_3H_3	FeC_2H	$FeCH_2$	C_5H_6	Fe	C_3H_3
$FeC_5H_6^+$								
cyclopentane		100.0	10.1	3.6	0.7	1.4	42.4	1.4
cyclopentadiene		100.0	7.0	3.7	0.7	1.8	36.0	1.5
$FeC_5H_8^+$								
cyclopentane	100	11.2	1.8	0.7	0.3	0.5	6.9	0.2
cyclopentene	100	7.6	1.2	0.5	0.3	0.4	4.7	0.2

Table VIII. CAD Spectra of $FeC_6H_{12}^+$

olefin	fragment ions														
	Fe-C_6H_{10}	Fe-C_6H_9	Fe-C_6H_6	Fe-C_5H_8	Fe-C_4H_8	Fe-C_4H_7	Fe-C_4H_6	Fe-C_3H_6	Fe-C_3H_5	Fe-C_3H_4	Fe-C_3H_3	Fe-C_2H_4	Fe-C_2H_3	$FeCH_3$	Fe
1-hexene	1.7	1.0		2.9	14.4	2.1	4.2	100.0	9.9		5.0	1.4	3.3	3.8	18.6
bis(propene)[a]	0.6	1.2						100.0	15.9		6.1		1.8	4.3	21.3
1-nonene	1.8	0.7		1.4	12.9	2.1	4.3	100.0	10.7		5.0	1.4	3.2	3.6	17.5
trans-2-hexene	2.9	0.7		4.3	100.0	7.1	17.3	2.9	1.4	1.4	1.4	7.9	5.0	2.5	11.2
cis-2-hexene	1.3	0.7		3.3	100.0	7.9	19.1	2.6	1.3	1.3	1.3	7.9	5.3	2.6	11.2
trans-4-octene	3.0	1.5		8.3	100.0	9.1	18.9	41.7	6.1		2.3	9.1	6.1	4.5	18.9
cis-4-octene	2.6	1.3		6.6	100.0	8.5	21.6	48.5	6.6		3.9	9.2	7.2	4.6	19.7
trans-3-hexene	2.0	1.0		6.2	100.0		16.6	3.5				8.2	5.0	2.7	9.9
cis-3-hexene	2.1	0.9		13.9	100.0		15.9	3.7				8.2	5.3	2.7	10.6
2-methyl-1-pentene	1.4	0.7		6.7	100.0	8.6		1.2	1.5	3.9	1.8	6.9	1.8	4.8	14.6
2-methyl-2-pentene	2.4	1.2		25.9	100.0	6.7		3.0	1.5	4.3	2.5	6.4	2.1	5.5	13.4
4-methyl-3-heptene	3.1	0.8		21.1	100.0	6.9		1.9	1.5	4.6	2.3	6.1	1.5	5.4	13.8
3-methyl-3-heptene	11.4	0.4		79.0	100.0	8.3	19.7	4.4	2.5	3.8	1.9	8.9	5.7	5.7	15.2
3-methyl-2-pentene	11.6			100.0	75.4		12.6	0.5		0.7		4.6	2.8	3.3	10.3
cyclohexane	100.0		19.0		2.0			3.2							22.5

[a] Formed by reaction of $Fe(CO)_2^+$ with propene.

CAD spectra of $Fe(C_5H_8)^+$ and $Fe(C_5H_6)^+$ produced by decomposition of the Fe(cyclopentane)$^+$ adduct may be compared with those of model complexes (Table VII). Loss of H_2 produces a complex with a CAD spectrum which matches that of Fe(cyclopentene)$^+$, not the acyclic diene complexes. Loss of a second H_2 gives a complex which is identical with the Fe(cyclopentadiene)$^+$ model. These structures are in accord with those prepared in reaction of Co^+ with cyclopentane.[15]

$FeC_6H_{12}^+$. The CAD spectra of the FeC_6H_{12} ions (Table VIII) fit a mechanism whereby an olefin complex, wherever possible, rearranges by the allylic insertion outlined in Scheme II. Reactions 7–9 show the bis(olefin) complexes resulting from rearrangement

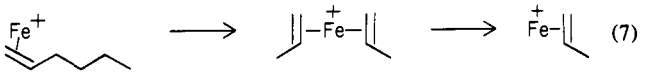

(7)

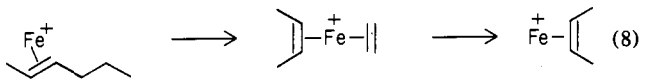

(8)

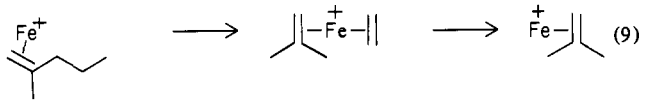

(9)

of Fe(1-hexene)$^+$, Fe(2-hexene)$^+$, and Fe(2-methyl-1-pentene)$^+$, respectively. The dominant fragment ion in the CAD spectra of these C_6H_{12} complexes is consistent with rearrangement to bis(olefin) complexes. For example, the CAD spectrum of Fe(1-hexene)$^+$ is quite similar to that of Fe(propene)$_2^+$ (Table VIII), which suggests that the 1-hexene complex primarily rearranges to the bis(propene) structure (reaction 7). Freiser and Jacobsen have recently reported that 1-hexene reacts with the Fe(1-hexene)$^+$ adduct to displace C_3H_6, which lends further support for the bis(propene) structure.[16] However, structures in addition to the bis(propene) complex are formed as indicated by the losses of CH_4 and C_2H_4 from Fe(1-hexene)$^+$.

In addition, the $FeC_3H_6^+$ and $FeC_4H_8^+$ products formed in the source can be identified by comparison of their CAD spectra with the corresponding reference spectra. The $FeC_3H_6^+$ ion from section 7 has a Fe(propene)$^+$ structure (Table V). The structure of the $FeC_4H_8^+$ ion produced in reactions 8 and 9 is Fe(butene)$^+$ and Fe(isobutene)$^+$, respectively (see Table III).

Note that while the CAD spectra of the 2-hexene and 2-methyl-1-pentene complexes are dominated by loss of ethylene, the $FeC_4H_6^+$ fragment is only present in the CAD spectrum of the 2-hexene complex. After the loss of ethylene (reaction 8), the butene complex may rearrange to a butadiene dihydrido complex by a mechanism similar to Scheme IV. Fe(2-methyl-1-pentene)$^+$ cannot form a stable butadiene complex without a complicated carbon skeletal rearrangement which would be in competition with the facile loss of ethylene via the allylic insertion mechanism.

For complexes where a β-H shift following insertion into the allylic C–C bond is *not* possible, rearrangements may now occur to form a new complex which can undergo a β-H shift. The complexes of 3-hexene and 2-methyl-2-pentene probably isomerize via the β-H atom shift mechanism (Scheme III). The bis(olefin) complex that results after isomerization accounts for the observed $FeC_4H_8^+$ products (see reactions 10 and 11). The CAD spectra

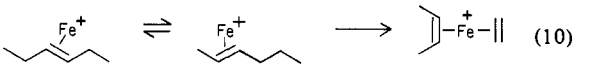

(10)

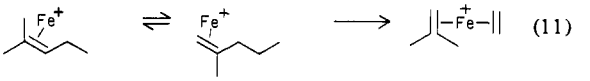

(11)

of the $FeC_4H_8^+$ produced by reactions of Fe^+ with 3-hexene and 2-methyl-2-pentene in the source were identical with the CAD spectra of the products from reactions 8 and 9, respectively.

The complex prepared from *cis*-3-methyl-2-pentene is the only $FeC_6H_{12}^+$ studied that loses CH_4 more readily than it loses a small olefin. A mechanism that accounts for this behavior is given in Scheme V. After insertion into the allylic C–C bond a hydrogen atom is transferred via a six-membered ring transition state, **11**, resulting in a hydrido methyl isoprene complex, **12**. The reductive elimination of CH_4 upon collisional activation of **12** would yield Fe(isoprene)$^+$. Indeed, the CAD spectrum of the $FeC_5H_8^+$

Table IX. CAD Spectra of Acyclic $FeC_5H_8^+$

olefin	fragment ions													
	Fe-C_5H_6	Fe-C_5H_5	Fe-C_4H_4	Fe-C_3H_6	Fe-C_3H_5	Fe-C_3H_4	Fe-C_3H_3	Fe-C_2H_4	Fe-C_2H_3	FeC_2H_2	FeC_2H	$FeCH_3$	$FeCH_2$	Fe
1,3-pentadiene	20.1	18.5	5.2	59.3	9.9	13.6	13.6			100.0	10.5	6.2	3.7	53.7
1,4-pentadiene	6.2	19.1	4.6	58.6	26.5	11.7	16.7			100.0		7.4	3.7	51.2
isoprene	27.5	13.6	74.7	49.4	20.4	52.4	26.5	4.0	18.5	75.3	15.4	11.7	6.8	100.0
3-methyl-2-pentene	24.5	18.2	65.7	41.3	23.1	46.2	26.6	4.2	18.2	62.2	14.0	11.9	6.3	100.0

Table X. CAD Spectra of $FeC_6H_{10}^+$

hydrocarbon	fragment ions											
	FeC_6H_9	FeC_6H_8	FeC_6H_7	FeC_6H_6	FeC_5H_5	FeC_4H_8	FeC_4H_6	FeC_3H_6	FeC_3H_4	FeC_3H_3	FeC_2H_3	Fe
cyclohexane		21.4	7.3	100.0								7.3
cyclohexene		47.8	5.7	100.0								5.7
1,5-hexadiene	8.0	16.0	17.3	11.1	8.6	14.8	32.1	15.4	100	24.1	17.3	50.6

Table XI. CAD Spectra of $FeC_6H_6^+$

hydrocarbon	fragment ions									
	FeC_6H_5	FeC_6H_4	FeC_4H_4	FeC_4H_3	FeC_3H_3	FeC_3H_2	FeC_2H	C_6H_6	Fe	C_4H_3
cyclohexane	100.0	26.7		14.3		2.5	27.3	5.0	97.8	1.9
benzene	60.0	8.5		12.3		2.7	22.5	0.6	100.0	2.3
1,3,5,7-cyclooctatetraene	83.3	14.2		16.4		3.1	27.8	4.9	100.0	2.5
$Fe(CO)_3$-cyclohexadiene	99.3	11.9		16.8		3.0	26.1	6.0	100.0	2.6
1,5-hexadiyne	47.8	58.5	60.4	23.3	22.0	22.6	47.1	1.9	100.0	1.3

Scheme V

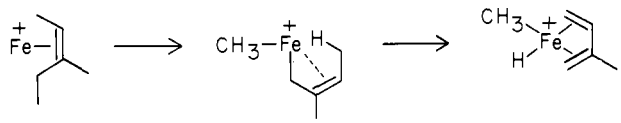

11 **12**

formed by decomposition of Fe(3-methyl-2-pentene)$^+$ matches that of the complex prepared with isoprene but is significantly different than those of the complexes involving linear pentadienes (Table IX).

The other large fragment in the CAD spectrum of Fe(3-methyl-2-pentene)$^+$ is formed by the loss of ethylene. Isomerization of the olefin complex by a β-H shift would result in the bis(olefin) complex (reaction 12) which, in the source, decomposes to $FeC_4H_8^+$ which gives a CAD spectrum identical with that of Fe(butene)$^+$ (Table III).

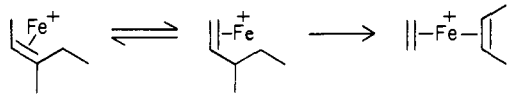

(12)

The mechanism for the loss of methane (Scheme V) also accounts for this loss from the 2-pentene, 2-methyl-2-pentene, and 3-hexene complexes. For Fe(2-methyl-2-pentene)$^+$, loss of CH_4 is 4 times more intense than for the 2-methyl-1-pentene complex. In order to lose methane by the mechanism in Scheme V, isomerization of the 2-methyl-1-pentene complex to Fe(2-methyl-2-pentene)$^+$ is required. The isomerization must be less facile than the allylic insertion shown in reaction 9. The more abundant loss of methane shown in the CAD spectrum of *cis*-3-hexene compared to that of the trans complex may also be explained by this mechanism. The methane loss involving a cis intermediate, **13**, would be expected to be more facile for steric reasons than for a trans intermediate, **14**. Furthermore, the more abundant loss

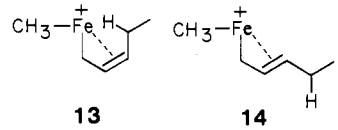

13 **14**

of methane from the 3-hexene than from the 2-hexene complexes can also be explained by the same mechanism.

The CAD spectrum of Fe(cyclohexane)$^+$ is dominated by dehydrogenation (reactions 13 and 14). The cleavage of C–H

$$FeC_6H_{12}^+ \rightarrow FeC_6H_{10}^+ + H_2 \quad (13)$$

$$FeC_6H_{12}^+ \rightarrow FeC_6H_6^+ + 3H_2 \quad (14)$$

bonds in the cycloalkane complex contrasts with the allylic C–C cleavage observed in the olefin complexes. The CAD spectrum of the Fe(C_6H_{10})$^+$ product from reaction 13 compares well with that of the cyclohexene complex but is definitely dissimilar to the CAD spectrum of Fe(1,5-hexadiene)$^+$ (see Tables X and XI). The CAD spectrum of Fe(C_6H_6)$^+$ from reaction 14 is very similar to the spectrum of Fe(benzene)$^+$ and the spectra of the $FeC_6H_6^+$ ion formed by electron ionization of cyclohexadiene iron tricarbonyl (reaction 15), and by reaction of Fe$^+$ with 1,3,5,7-cyclooctatetraene (reaction 16). All produce a common $FeC_6H_6^+$ product, presumably Fe(benzene)$^+$.

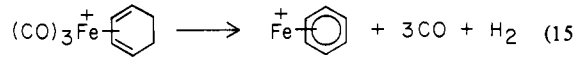

(15)

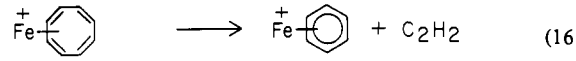

(16)

Test of Mechanism

Study of $FeC_8H_{16}^+$. The octene and methylheptene isomers were chosen to test the preferential insertion of Fe$^+$ into the allylic C–C bond. If all of the isomers give intermediates analogous to **6** in Scheme II, then products shown in reactions 17–20 would be

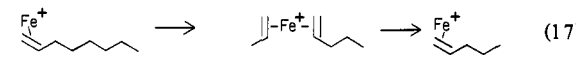

(17)

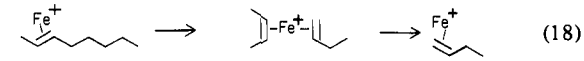

(18)

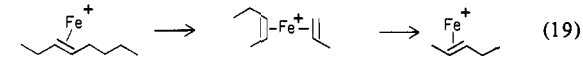

(19)

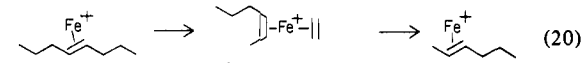

(20)

Table XII. CAD Spectra of $FeC_8H_{16}^+$

olefin	fragment ions											
	Fe-C_8H_{14}	Fe-C_7H_{12}	Fe-C_6H_{12}	Fe-C_6H_{10}	Fe-C_5H_{10}	FeC_5H_8	FeC_4H_8	FeC_4H_6	FeC_3H_6	FeC_3H_4	FeC_2H_4	Fe
1-octene	2.9		5.5	0.5	100.0	5.4	5.6	10.6	26.8		5.4	12.5
cis-2-octene	9.9	0.6	8.2		6.6	2.0	100.0	30.2	3.6		8.3	13.9
trans-2-octene	11.8	0.6	9.8		7.5	2.5	100.0	29.8	3.9		8.6	13.8
cis-3-octene	8.6	4.0	51.8	2.8	100.0	13.8	30.1	22.2	28.1		6.4	16.5
trans-3-octene	10.3	2.7	59.4	3.4	100.0	14.8	61.6	29.1	30.9		9.5	21.4
cis-4-octene	1.5	0.7	100.0	5.2	10.8	4.9	17.1	7.3	8.0	3.3	3.3	7.5
trans-4-octene	3.8	1.2	100.0	3.7	29.7	8.6	22.7	10.4	13.5	4.2	4.2	10.6
2-methyl-1-heptene	6.1	0.5	3.7		2.4	1.4	100.0	15.6				14.3
2-methyl-2-heptene	10.6	6.1	25.8	3.8	100.0	23.9	32.6	25.0	29.9		4.5	18.9
cis-3-methyl-3-heptene	10.0	27.1	100.0	14.0	80.3	50.2	26.4	28.1	24.1		6.7	19.1
4-methyl-3-heptene	3.6	9.1	100.0	11.7	9.5	22.6	22.6	4.4	5.8	6.6	4.7	8.8

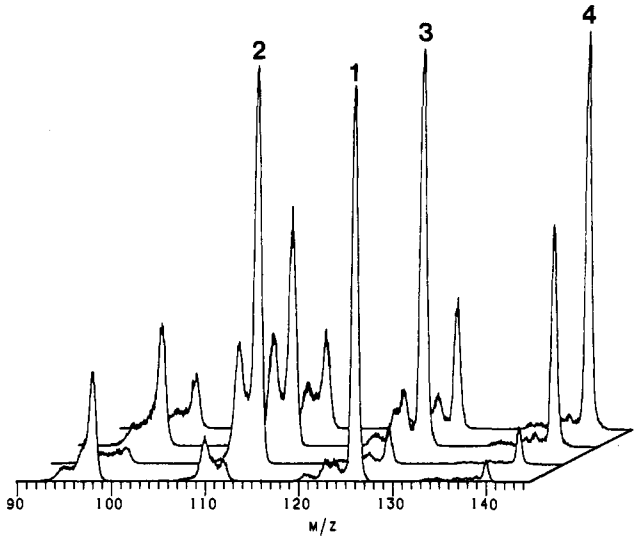

Figure 5. Partial CAD spectra of $FeC_8H_{16}^+$, m/z 168: (1) $FeC_5H_{10}^+$, m/z 126, from 1-octene; (2) $FeC_4H_8^+$, m/z 112, from *trans*-2-octene; (3) $FeC_5H_{10}^+$, m/z 126, from *trans*-3-octene; and (4) $FeC_6H_{12}^+$, m/z 140, from *trans*-4-octene.

expected upon collisional activation of the various Fe(octene)$^+$ isomers. As shown in Figure 5, the largest peak in each spectrum corresponds to the loss predicted for the allylic insertion mechanism (see Table XII for full CAD spectra). Furthermore, the cis and trans isomers of 3- and 4-octene may be distinguished by the CAD spectra of their complexes with Fe^+ (see Figure 6).

If the allylic insertion mecanism is general, the methylheptene complexes should dissociate to give the products shown in reactions 21–24. The predicted losses are in fact the major products

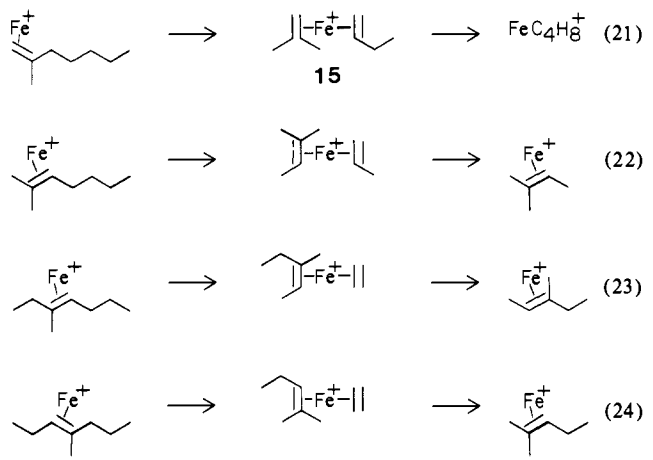

observed in the CAD spectra of the methylheptene complexes (see Figure 7).

Study of Products from Decomposition of $FeC_8H_{16}^+$. CAD spectroscopy affords the opportunity to investigate the product

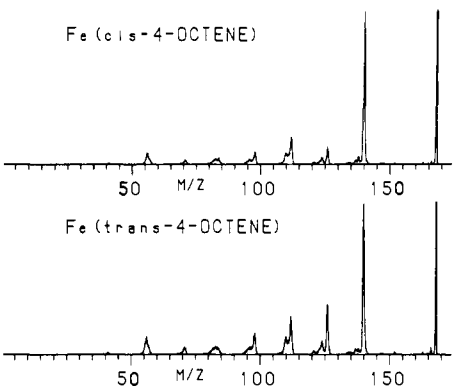

Figure 6. CAD spectra of $FeC_8H_{16}^+$ from *cis*-4-octene and *trans*-4-octene.

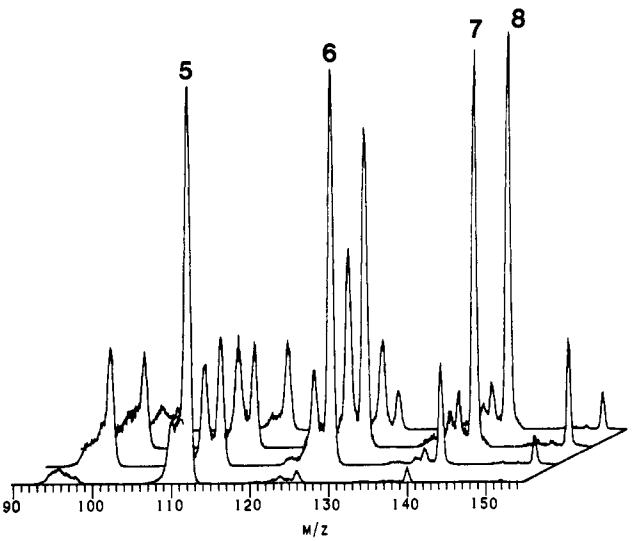

Figure 7. Partial CAD spectra of $FeC_8H_{16}^+$, m/z 168: (5) $FeC_4H_8^+$, m/z 112, from 2-methyl-1-heptene; (6) $FeC_5H_{10}^+$, m/z 126, from 2-methyl-2-heptene; (7) $FeC_6H_{12}^+$, m/z 140, from 3-methyl-3-heptene; and (8) $FeC_6H_{12}^+$, m/z 140, from 4-methyl-3-heptene.

ions formed either by decomposition of the $FeC_8H_{16}^+$ complexes in the CI source (MS/MS) or by collisional activation of the $FeC_8H_{16}^+$ isomers (MS/MS/MS). CAD spectra of these product ions serve as further test of the allylic insertion mechanism. For example, as indicated in reaction 17, CAD of Fe(1-octene)$^+$ gives predominantly a $FeC_6H_{12}^+$ fragment. The CAD spectrum of $FeC_6H_{12}^+$ as determined by an MS/MS/MS experiment matches that of Fe(1-hexene)$^+$. This result provides verification of the unimolecular rearrangement of the bis(olefin) complex by the allylic insertion mechanism as indicated in reaction 17. Similarly, consecutive reaction experiments on the products of reactions 18–24 verify the proposed structures. The reaction of 1-octene with Fe^+ in the source also produces a $FeC_6H_{12}^+$ product which is identical with Fe(1-hexene)$^+$. Thus, both unimolecular rear-

Table XIII. Partial CAD Spectra of Fe(1-alkenes)$^+$

	neutral loss															
olefin	H_2	C_2H_4	C_3H_6	C_3H_8	C_4H_8	C_5H_{10}	C_6H_{12}	C_6H_{14}	C_7H_{14}	C_7H_{16}	C_8H_{16}	C_8H_{18}	C_9H_{18}	$C_{10}H_{20}$	$C_{11}H_{22}$	$C_{12}H_{24}$	$C_{14}H_{28}$
1-heptene	2.7	3.4	100	24.1	29.7	7.6			17.9								
1-nonene	3.4	3.4	100	2.7	4.1	9.5	25.3						9.1				
1-decene	4.4	3.5	100	1.9	6.0	9.5	19.3	10.1	13.9					7.6			
1-dodecene	6.5	4.5	100	3.2	3.2	14.6	53.2		8.4	9.7	16.2	15.6	21.4	7.1		7.1	
1-tetradecene	9.2	7.0	100		4.2	11.3	55.6	17.6	11.3		23.3	14.1	31.0	24.6	26.1	9.2	10.6

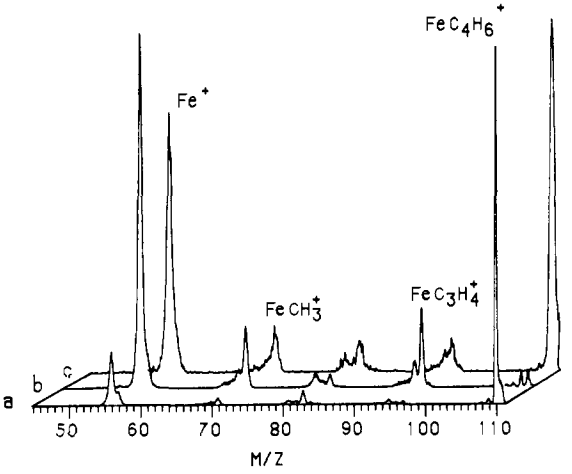

Figure 8. Partial CAD spectra of $FeC_4H_8^+$ from (a) 1-butene, (b) isobutene, and (c) MS/MS/MS of 2-methyl-1-heptene.

rangement of stable $FeC_8H_{16}^+$ and bimolecular reactions between Fe^+ and C_8H_{16} proceed by the allylic insertion mechanism. The fact that the complexes rearrange unimolecularly, even if they have sufficient energy to decompose, suggests the mechanism is a low-energy pathway without large internal energy barriers. Since the CAD spectra obtained by the MS/MS/MS experiment match those of the products of ion–molecule reactions, only the latter are tabulated as discussed below.

The $FeC_4H_8^+$ products of the ion–molecule reactions of Fe^+ with the C_8H_{16} isomers are presented in Table III. The product from reaction 18 is an Fe(butene)$^+$ complex as expected, not the isomeric isobutene complex. The partial CAD spectrum of $FeC_4H_8^+$ formed by collisional activation of Fe(2-methyl-1-heptene)$^+$ is a mixture of the CAD spectra of butene and isobutene complexes (see Figure 8). In fact, both losses of butene or isobutene are possible from **15**, the bis(olefin) complex produced in reaction 21, which results in a mixture of $FeC_4H_8^+$ structures. This provides a striking example of the sensitivity of the CAD technique to detect a mixture of ions and to provide additional evidence in support of the allylic insertion mechanism.

The CAD spectra of the $FeC_5H_{10}^+$ products from reactions 17, 19, and 22 can be compared with those of reference C_5H_{10} complexes (Table VI). The product from reaction 17 is Fe(1-pentene)$^+$, whereas reaction 19 gives a mixture of 1-pentene and 2-pentene complexes. The product from reaction 22 is possibly a mixture of methylbutene complexes but is definitely not a linear pentene complex.

The CAD spectra of $FeC_6H_{12}^+$ products from reactions 20, 23, and 24 can be compared in Table VIII with the corresponding reference spectra. The product from reaction 20 is a mixture of Fe(2-hexene)$^+$ and Fe(1-hexene)$^+$. On the basis of the CAD spectra, the product from reaction 23 is assigned to be Fe(3-methyl-2-pentene)$^+$ whereas the product from reaction 24 is Fe(2-methyl-2-pentene)$^+$. These structural assignments are in accord with the allylic insertion mechanism.

While the products shown in reactions 17–24 are the major structures of the complexes of Fe^+ and C_8H_{16} isomers, other structures must be invoked to account for the other fragments in each CAD spectrum. The allylic hydrogen atom shift mechanism shown in Scheme III accounts for the secondary CAD fragment ions from the 3-octene, 4-octene, and *cis*-3-methyl-3-heptene complexes. The rearrangement of the 3-octene complexes to a 2-octene or 4-octene complex is consistent with the large $FeC_6H_{12}^+$ and $FeC_4H_8^+$ fragments observed. Furthermore, the $FeC_4H_8^+$ fragment is twice as large in the CAD spectrum of Fe(*trans*-3-octene)$^+$ than in that of the cis complex. This suggests that the trans complex isomerizes more readily to the 2-octene complex than does Fe(*cis*-3-octene)$^+$. Similarly the isomerization of the 4-octene complexes to Fe(3-octene)$^+$ results in a large $FeC_5H_{10}^+$. Again the trans complex fragments to give a larger $FeC_5H_{10}^+$ fragment than does the cis complex.

The most intense fragment in the CAD spectrum of Fe(3-methyl-3-heptene)$^+$ corresponds to the loss of C_2H_4 by the allylic insertion mechanism (reaction 23). The loss of C_3H_6 is nearly as intense as the C_2H_4 loss and probably occurs as shown in reaction 25.

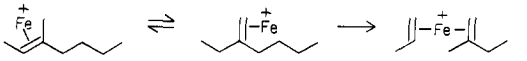

(25)

Isomerization of the double bond followed by the allylic insertion mechanism gives rise to the observed $FeC_5H_{10}^+$ product. The Fe(2-methyl-1-butene)$^+$ structure is assigned to the $FeC_5H_{10}^+$ product based on a comparison of CAD spectra (Table VI).

Other Fe(C_nH_{2n})$^+$. The CAD spectra of the complexes of Fe^+ with other selected 1-alkenes are summarized in Table XIII. All of the complexes principally lose C_3H_6 as predicted by the allylic insertion mechanism. The complexes of dodecene and tetradecene lose a second C_3H_6 presumably by a consecutive allylic insertion and β-H atom shift following the initial loss of propene.

Conclusion

Oxidative addition of the allylic C–C bond to the metal ion is facile in reactions of Fe^+ with olefins. This is the dominant process even in large olefins where addition of other bonds is energetically possible and statistically favorable. Following the addition, a β-hydrogen is transferred from the alkyl group to the metal and ultimately to the allyl fragment to produce a bis(olefin) complex. Upon activation, the complex loses the smaller olefin preferentially. If no β-H is available on the alkyl ligand, at least two alternative processes may occur. (1) A 1,3 shift of an allylic H atom effects a 1,2 shift of the double bond. Addition to the allylic C–C bond may then result in the formation of a bis(olefin) complex. (2) Loss of methane from complexes with no available β-H occurs possibly by a six-membered cyclic transition state.

The strained C–C bonds in the three- and four-membered rings add to Fe^+ to form metallacyclic and carbenoid structures. The five- and six-membered cycloalkanes react with Fe^+ via oxidative addition of the C–H bonds, and the integrity of the ring is retained.

The interaction between Fe^+ and a complexed olefin is extensive and very sensitive to structure. As a consequence, it is possible to distinguish between cyclic and acylic isomers, to locate double bonds in substituted olefins, and to identify differences in the behavior of cis and trans isomers as shown in this investigation. Some of these distinctions would be impossible with ion–molecule reactions involving an organic reagent ion alone and would probably be nearly as difficult with CAD in the low-energy regime where fewer reactions are observed. Thus, high-energy CAD may be uniquely suited to structural determination of gas-phase metal ion complexes. The investigation of the analytical applications of this chemistry is currently being pursued.

Acknowledgment. The NSF is acknowledged for partial support of this work (CHE 8110516 to D.P.R. and CHE 8008008 to

M.L.G.). The instrumentation is supported by a NSF Regional Instrumentation Facility Grant to the University of Nebraska (CHE 8211164).

Registry No. 1, 90823-18-0; **2**, 90823-19-1; **3**, 90823-20-4; **4**, 90823-21-5; **5**, 90823-22-6; **6**, 90823-23-7; **7**, 90823-24-8; **8**, 90823-25-9; **9**, 90823-26-0; **10**, 90823-27-1; **12**, 90823-28-2; Fe(1-heptene)$^+$, 90823-29-3; Fe(1-nonene)$^+$, 90823-30-6; Fe(1-decene)$^+$, 90823-31-7; Fe(1-dodecene)$^+$, 90823-32-8; Fe(1-tetradecene)$^+$, 90823-33-9; $Fe(CO)_5$, 13463-40-6; $Fe(CO)_2^+$, 35038-15-4; $Fe(CO)^+$, 35038-14-3; Fe^+, 14067-02-8; 1-hexene, 592-41-6; 1-heptene, 592-76-7; 1-octene, 111-66-0; *trans*-2-octene, 13389-42-9; cyclobutane, 287-23-0; methylcyclopropane, 594-11-6; $(ethylene)_2$, 16482-32-9; 1-butene, 106-98-9; *cis*-2-hexene, 7688-21-3; *cis*-3-hexene, 7642-09-3; *cis*-3-methyl-2-pentene, 922-62-3; 1-heptene, 592-76-7; 2-methyl-1-heptene, 15870-10-7; isobutene, 115-11-7; 2-methyl-1-pentene, 763-29-1; 2-methyl-2-pentene, 625-27-4; cyclopropane, 75-19-4; propene, 115-07-1; 1-pentene, 109-67-1; 2-methyl-1-butene, 563-46-2; 3-methyl-1-butene, 563-45-1; 2-methyl-2-butene, 513-35-9; *trans*-2-pentene, 646-04-8; *cis*-2-pentene, 627-20-3; *trans*-3-octene, 14919-01-8; *cis*-3-octene, 14850-22-7; 2-methyl-2-heptene, 627-97-4; cyclopentane, 287-92-3; bis(propene), 16813-72-2; 1-nonene, 124-11-8; *trans*-2-hexene, 4050-45-7; *trans*-4-octene, 14850-23-8; *cis*-4-octene, 7642-15-1; *trans*-3-hexene, 13269-52-8; 4-methyl-3-heptene, 4485-16-9; 3-methyl-3-heptene, 7300-03-0; 3-methyl-2-pentene, 922-61-2; cyclohexane, 110-82-7; 1,3-pentadiene, 504-60-9; 1,4-pentadiene, 591-93-5; isoprene, 78-79-5; 2-methyl-2-pentene, 922-61-2; cyclohexane, 110-83-8; 1,5-hexadiene, 592-42-7; benzene, 71-43-2; 1,3,5,7-cyclooctatetraene, 629-20-9; $Fe(CO)_3$-cyclohexadiene, 12152-72-6; 1,5-hexadiyne, 628-16-0; *cis*-2-octene, 7642-04-8; *cis*-3-methyl-3-heptene, 22768-18-9.

Determination of the Aluminum-27 Spin–Lattice Relaxation Rate and the Relative Number of Each Chloroaluminate Species in the Molten 1-*n*-Butylpyridinium Chloride/$AlCl_3$ System

T. Matsumoto and K. Ichikawa*

Contribution from the Department of Chemistry, Faculty of Science, Hokkaido University, Sapporo 060, Japan. *Received June 9, 1983*

Abstract: ^{27}Al longitudinal magnetization recovery curves were measured by using the inversion recovery method on molten 1-*n*-butylpyridinium chloride/$AlCl_3$ mixtures at various components of 39–80 mol % $AlCl_3$ and between 30 °C and 75 °C. The recovery curves did not show single exponential decays at the components located between the two stoichiometries (e.g., between 50 and 67 mol % $AlCl_3$), in contrast with the single exponential decays observed in melts at less than 50 mol % $AlCl_3$ and at 67 mol % $AlCl_3$. The composition dependence of the individual relaxation rates $R_{1,\alpha}$ and the individual concentrations X_α of each main chloroaluminate species, α, such as $AlCl_4^-$, $Al_2Cl_7^-$, $Al_3Cl_{10}^-$, or Al_2Cl_6, were obtained by fitting a model associated with the chemical exchange process from species A to B into the observed nonlinear logarithmic recovery curve. The remarkably slow exchange rate (i.e., the long exchange lifetime) was comparable with the relaxation rates in magnitude, and it gave rise to the nonlinear nature in the logarithmic recovery curves. The chemical exchange from species A to B promotes the individual relaxation of ^{27}Al in each species α. This is because the relaxation rate is the minimum in magnitude for the melt at the BPCl-rich side of 50 mol % $AlCl_3$ or at the stoichiometric composition, in which the chemical exchange from species A to B does not take place. Over all the compositions, the empirical rule among each $R_{1,\alpha}$ is as follows: $R_{1,AlCl_4^-} < R_{1,Al_2Cl_7^-}$, $R_{1,Al_2Cl_7^-} < R_{1,Al_3Cl_{10}^-}$, and $R_{1,Al_2Cl_6} < R_{1,Al_3Cl_{10}^-}$. Here the NMR relaxation of the ^{27}Al nucleus in the melts originates mainly from the interaction between the quadrupolar moment and the electric field gradient fixed at a central Al nucleus by sharing electrons with the chlorines of the nearest neighbors in each species. The dependence of the mole fractions $X(AlCl_4^-)$ and $X(Al_2Cl_7^-)$ of the $AlCl_4^-$ and $Al_2Cl_7^-$ species on the formal composition was consistent with the potentiometric and Raman spectra investigations. Above 67 mol % $AlCl_3$, the other $Al_3Cl_{10}^-$ and Al_2Cl_6 species are present as the main species: a probable peak in the $X(Al_3Cl_{10}^-)$ values locates near the stoichiometry $BPAl_3Cl_{10}$ (or 75 mol % $AlCl_3$), and above 75 mol % $AlCl_3$, the Al_2Cl_6 species becomes a main species upon successive additions of the $AlCl_3$ component.

Considerable interest has been shown recently in chloroaluminate melts such as $AlCl_3$/MCl (M = Li, Na, etc.) and $AlCl_3$/alkylpyridinium halide because of their special properties as acid–base solvents.[1] Raman spectroscopic studies have shown that $AlCl_4^-$, $Al_2Cl_7^-$, $Al_nCl_{3n+1}^-$ ($n \geq 3$), and Al_2Cl_6 are present in their melts.[2,3] The anionic species equilibrium for the dissociation reaction

$$2AlCl_4^- \rightleftarrows Al_2Cl_7^- + Cl^-$$

has been investigated by potentiometry.[4,5] ^{27}Al nuclear magnetic resonance studies on chloroaluminate melts have examined the characteristics of these melts, which consist of the $AlCl_4^-$ and $Al_2Cl_7^-$ ions.[6] To our knowledge, the relaxation phenomena on the ^{27}Al longitudinal and transverse magnetizations have not been investigated, though the ^7Li and ^{23}Na spin–lattice relaxation rates have been obtained in molten $LiAlCl_4$ and $NaAlCl_4$, respectively.[7]

This paper describes an examination of the formal composition dependence of the individual relaxation rates, $R_{1,\alpha}$, and of the mole fractions, X_α, of the main species such as $AlCl_4^-$, $Al_2Cl_7^-$, Al_2Cl_6 and a high polymer assigned tentatively to $Al_3Cl_{10}^-$ by measuring the ^{27}Al longitudinal magnetization recovery curves for the room-temperature melt of 1-*n*-butylpyridinium chloride (BPCl) + $AlCl_3$ mixtures and by reproducing the experimental recovery

(1) Boston, C. R. "Advances in Molten Salt Chemistry"; Braunstein, J., Mamantov, G., Smith, G. P., Eds.; Plenum Press: New York, 1971; Vol. 1, p 219. Jones, H. L.; Osteryoung, R. A. "Advances in Molten Salt Chemistry"; Plenum Press: New York, 1975; Vol. 3, p 121. Chum, H. L.; Osteryoung, R. A. "Ionic Liquid"; Inman, D., Lovering, D. G., Eds.; Plenum Press: New York, 1981; p 407.
(2) Gale, R. J.; Gilbert, B.; Osteryoung, R. A. *Inorg. Chem.* **1978**, *17*, 2728.
(3) Rytter, E.; Øye, H. A.; Cyvin, S. J.; Cyvin, B. N.; Klaeboe, P. J. *Inorg. Nucl. Chem.* **1973**, *35*, 1185.
(4) Gale, R. J.; Osteryoung, R. A. *Inorg. Chem.* **1979**, *18*, 1603.
(5) Torsi, G.; Mamantov, G. *Inorg. Chem.* **1971**, *11*, 1439.
(6) Gray, J. L.; Maciel, G. E. *J. Am. Chem. Soc.* **1981**, *103*, 7147.
(7) Matsumoto, T.; Ichikawa, K. *Bull. Chem. Soc. Jpn.* **1982**, 1100.

0002-7863/84/1506-4316$01.50/0